Supplementary Materials for

Organic Synthesis via Irradiation and Warming of Ice Grains in the Solar Nebula

Fred J. Ciesla* and Scott A. Sandford

*To whom correspondence should be addressed. E-mail: fciesla@uchicago.edu

This PDF file includes:

Supplementary Text
Figs. S1 to S11
Full Reference List

Supplementary Text

1. Model Description

Protoplanetary disks are dynamic objects through which mass is accreted onto the central star during the final stages of that star's formation. This evolution is controlled by processes which generate an effective viscosity, ν, and stresses within the differentially rotating gas of the disk. In the thin-disk approximation, the surface density, Σ, of the gas then evolves as described by (32):

$$\frac{\partial \Sigma}{\partial t} = -\frac{1}{r}\frac{\partial}{\partial r}\left(r\Sigma v_g\right) \tag{1}$$

where v_g is the velocity of the gas flow in the radial direction. In the case of disks which are in steady-state, the velocity is given by:

$$v_g = -\frac{3\nu}{2r} \tag{2}$$

The dynamical evolution of solids in the solar nebula were determined by turbulent diffusion (where turbulence was present), gravitational settling, gas drag, and the large-scale motions associated with disk evolution. In the case of radial motions, the motions of a collection of solids of a given size can be described by:

$$\frac{\partial \Sigma_i}{\partial t} = \frac{1}{r}\frac{\partial}{\partial r}\left(r\Sigma D_i\frac{\partial}{\partial r}\left(\frac{\Sigma_i}{\Sigma}\right)\right) - \frac{1}{r}\frac{\partial}{\partial r}\left(rv_r\Sigma_i\right) \tag{3}$$

where Σ_i is the surface density of the solids of interest, D_i is the diffusivity that arises due to turbulence, and v_r are the radial velocity of the solids from the advective motions of the gas and gas drag that arises from radial pressure gradients (33). The extent to which solids are pushed by the gas (either by turbulence or gas drag) is quantified by the dimensionless stopping time, τ, which is given by:

$$\tau = \left(\frac{\rho a}{\rho_g c_s}\right)\Omega \tag{4}$$

where ρ is the material density of the solids, a is the radius of the particles of interest, ρ_g is the local gas density, c_s is the local speed of sound in the gas, and Ω is the local Keplerian rotation rate. The term in parentheses is the traditional stopping time–a measure of the amount of time a particle would take to lose its relative velocity with respect to the gas. Given a value of τ, the diffusivity of the solid species would be given by (34):

$$D_i = \frac{D_g}{1 + \tau^2} \tag{5}$$

where D_g is the diffusivity of gaseous species in the disk. As a first-order approximation, we make the common assumption that $D_g \sim \nu$. This is not far off where viscosity is driven by the magnetorotational instability (MRI) when the gas diffusivity and viscosity may differ by a factor of a few (35).

In defining the radial velocity of the solids, we follow (*36*), and use:

$$v_r = \frac{v_g \tau^{-1} - \eta v_K}{\tau + \tau^{-1}} \tag{6}$$

where η is a term that relates the pressure supported orbital velocity of the gas $v_{\phi,g}$ to the keplerian orbital velocity, v_K by:

$$v_{\phi,g}^2 = v_K^2 (1 - \eta) \tag{7}$$

In our model, as solids are allowed to diffuse vertically, we calculate η based on the radial pressure gradient at the height of the particle using:

$$\eta = -\frac{r}{\rho_g v_K^2} \frac{\partial P}{\partial r} \tag{8}$$

where ρ_g and $\frac{\partial P}{\partial r}$ are evaluated at both the radial and vertical locations of the particle.

In the vertical direction, that is the direction perpendicular to the disk midplane, the gas is assumed to be in hydrostatic equilibrium. This means the gas will follow a gaussian distribution where $\rho_g (z) = \rho_g (z = 0) \exp\left(-\frac{z^2}{2H^2}\right)$. The vertical motions of a distribution of solid particles in a disk are described by the equation describing the volume density of solids, ρ_i:

$$\frac{\partial \rho_i}{\partial t} = \frac{\partial}{\partial z}\left(\rho_g D_i \frac{\partial}{\partial z}\left(\frac{\rho_i}{\rho_g}\right)\right) - \frac{\partial}{\partial z}(\rho_i v_z) \tag{9}$$

Here we assume the vertical diffusivity is comparable to the radial diffusivity, though differences may arise (*35*). The vertical velocity of the solids, v_z, is determined by balancing the vertical component of the gravitational force from the central star with the drag force caused by the movement of the solid through the gaseous fluid. This yields:

$$v_z = -\tau \Omega z \tag{10}$$

Equations (3) and (9) are typically solved using finite difference methods, tracking how the density of materials in a disk evolves as a function of time and location. In this study, we use particle tracking techniques (*13-15*) which allow us to follow the paths of individual particles whose motions are governed by the same processes that determine the forms of Equations (3) and (9). The equations which describe the motions of the solids are thus:

$$x_i = x_{i-1} + v_{eff,x}\delta t + \psi \left[\frac{2}{\xi}D_i (x') \delta t\right]^{\frac{1}{2}} \tag{11}$$

$$y_i = y_{i-1} + v_{eff,y}\delta t + \psi \left[\frac{2}{\xi}D_i (y') \delta t\right]^{\frac{1}{2}} \tag{12}$$

$$z_i = z_{i-1} + v_{eff,z}\delta t + \psi \left[\frac{2}{\xi}D_i (z') \delta t\right]^{\frac{1}{2}} \tag{13}$$

2

Where we have adopted Cartesian coordinates, x and y to describe the radial motions of the particles, relating these coordinates to the cylindrical radius by $r^2 = x^2 + y^2$.

The equations above allow us to calculate the new position of a particle (r_i, z_i) from its old position (r_{i-1}, z_{i-1}) after a timestep δt. The second terms in the equations each contain a velocity, v_{eff} which include the velocities in the equations (3) and (9) above from gas drag, disk evolution, or gravitational settling (in the case of x and y, broken into their respective components, e.g., $v_{eff,x} = v_r \frac{x_{i-1}}{r_{i-1}}$). These velocities were augmented by additional advective terms to account for spatial gradients in gas density and diffusivity (derivations and explanations for these terms are given in *13-15*).

The third term in each equation represents the random displacement of the particles from turbulence. This term is determined by determining a random number, ψ, from a distribution with variance, ξ. The diffusivity is evaluated at a point slightly displaced from the previous location in the direction of increasing diffusivity, e.g. $z' = z_{i-1} + \frac{1}{2} \frac{\partial D_i}{\partial z} \delta t$. Here we used a uniform distribution of random numbers ranging from -1 to 1, with a variance $\xi = \frac{1}{3}$.

Tests of this particular model were performed (*13,14*)) to ensure that the particle tracking models produced results consistent with the finite volume solutions of the advective-diffusive equations.

2. Details of Particle Transport and Irradiation

Figure 3 of the main manuscript presented a scatter plot of the irradiation histories of the surviving particles in our primary model against their locations after 10^6 years of evolution. Figures S1 and S2 show the radial distribution of these particles in greater detail. The surface density of particles is traditionally what is shown when tracking the radial distribution of materials in an evolving protoplanetary disk. The initial distribution of particles would have been a delta function at $r = 49$ AU. As can be seen in Fig. S2, the materials in the disk spread throughout the disk, but the peak in the distribution migrates inwards as expected for a steady-state disk whose net motions are inward (Eq. 2).
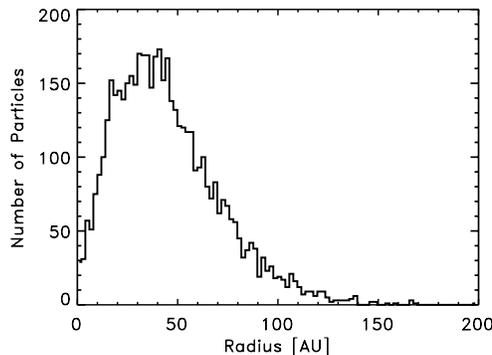

Fig. S1. Histogram showing the final location of the surviving particles for the 1 μm particles as discussed in the primary manuscript.
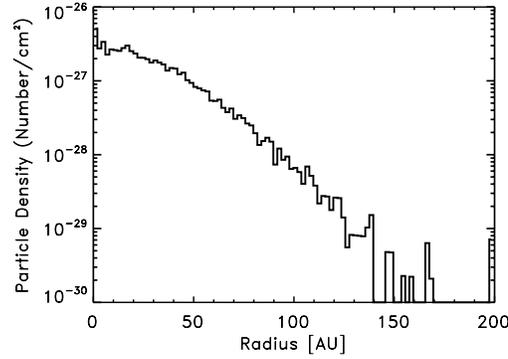
Fig. S2. A plot of the surface density of particles after 10^6 years of evolution in the disk. The surface density was determined by taking the histogram in Fig. S1 and dividing each radial bin which contained particles by its area. Thus the resulting density is the number of particles in each annulus in the disk divided by the area of the annulus.

The irradiation of the particles in our model occur when they are lofted to high altitudes of the disk as described in the main manuscript. This is why the irradiation histories shown in Figure 2 increase episodically. Figure S3 shows that the episodic increases in incident photons correspond to those times when the particles are lofted to significant heights in the disk, as discussed in the main manuscript.
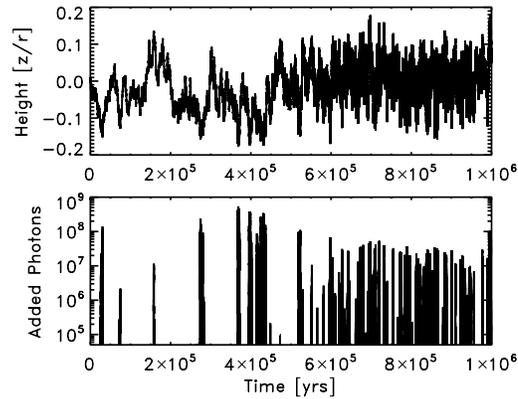

Fig. S3. The top panel here shows the height above the disk midplane of the particle shown in our Figure 1, divided by the distance from the Sun (z/r; a measure of relative height in the disk). The bottom panel shows the number of photons added to the cumulative number for that particle. As can be seen, photons are added when the particles reach relatively high distances above the disk midplane, as we expect. Note not all z/r excursions are equal as particles spend longer times there in the outer disk due to the longer dynamical timescales and thus see high UV fluxes for a longer period of time, for example.

3. Additional Results

Here we show the results of the 1 μm particles as considered in the main manuscript, along with those particles measure 10 μm, 100 μm, and 1 mm in diameter in Figures 1-4, respectively. In each case, the initial conditions were as described in the main manuscript, and we tracked the dynamics of 5000 particles of each size. We plot the final radial position of all surviving particles (those that do not migrate inward of 0.1 AU from the Sun) and the total cumulative number of UV photons the particles saw in the nominal case considered here.
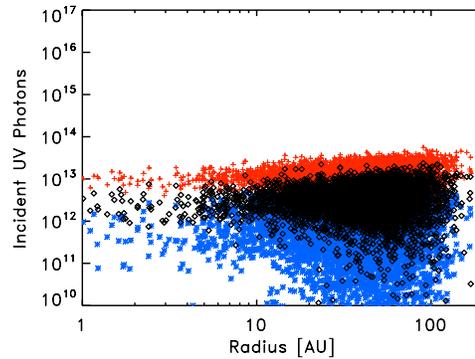

Fig. S4. The total number of incident photons for each of the 4979 surviving 1 μm grains plotted against their final location after 10^6 years of evolution (black diamonds). The light red plus signs and blue asterisks represent the same calculations using the lower and higher opacities as described in the main manuscript.
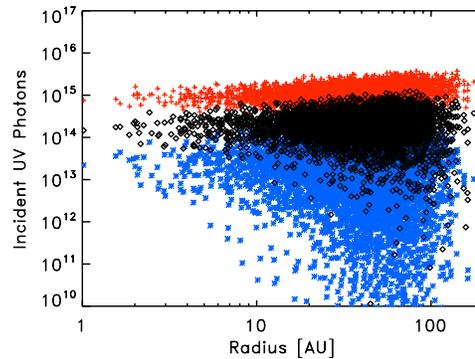

Fig. S5. The total number of incident photons for each of the 4975 surviving 10 μm grains plotted against their final location after 10^6 years of evolution (black diamonds). The light red plus signs and blue asterisks represent the same calculations using the lower and higher opacities as described in the main manuscript.

Fig. S6. The total number of incident photons for each of the 4937 surviving 100 μm grains plotted against their final location after 10^6 years of evolution (black diamonds). The light red plus signs and blue asterisks represent the same calculations using the lower and higher opacities as described in the main manuscript.
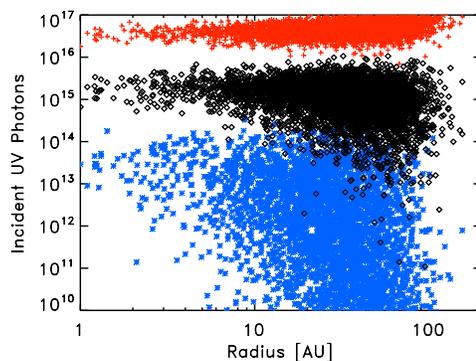

Fig. S7. The total number of incident photons for each of the 3160 surviving 1 mm grains plotted against their final location after 10^6 years of evolution (black diamonds). The light red plus signs and blue asterisks represent the same calculations using the lower and high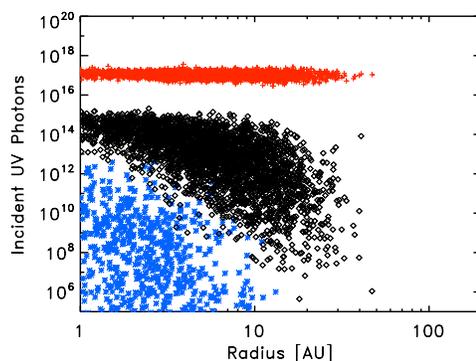er opacities as described in the main manuscript. The effects of gas drag are readily seen in this case, as the millimeter-sized particles drift inward $\sim 10\times$ faster than the smaller grains. These grains thus are concentrated at smaller radial distances, and have a smaller fraction of survivors.

The larger particles receive, on average, the greatest cumulative dosage of UV photons. However, these larger particles contain a greater number of ice molecules, which would dilute the efficiency of organic production. As discussed in the main manuscript, the key value here in determining organic production is the number of photons per molecule. Figures 5-8 plot this value for the surviving particles shown in Figures 1-4.

Comparison of these results shows that while the larger particles receive a greater total
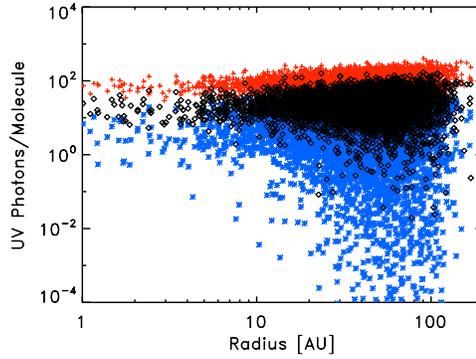
6

Fig. S8. The total UV photons per ice molecule in the surviving 1 μm grains plotted against their final location after 10^6 years of evolution. Colored symbols are as above.

Fig. S9. The total UV photons per ice molecule in the surviving 10 μm grains plotted against their final location after 10^6 years of evolution. Colored symbols are as above.
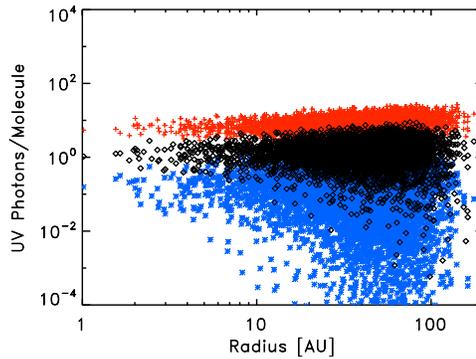
number of UV photons, there is also a larger number of molecules to which can be broken by those photons. Given that ∼1 organic molecule is created per 400 incident photons, the fraction of ice that is converted to organics is less in these larger particles than the smaller particles. Thus we expect the smaller particles to be the primary carriers for organics.

What is also apparent here is the effect that size has on the dynamical evolution of the solids. Small particles which are coupled to the gas, those with $\tau << 1$, will drift inward with roughly the velocity of the gas. Gas drag will augment this inward velocity, but is a strong function of τ. The initial value of τ for the particles considered here (at their starting positions) are: ∼6×10^{-6}, 6×10^{-5}, 6×10^{-4}, and 0.006 respectively. Thus gas drag will be most important for the millimeter-sized particles, with diminishing importance for the other sizes. This effect is readily seen as the radial expanse of the millimeter swarm of particles is much less than for the other particles, and as fewer particles survive the effects of inward drift over the 1 Myr period
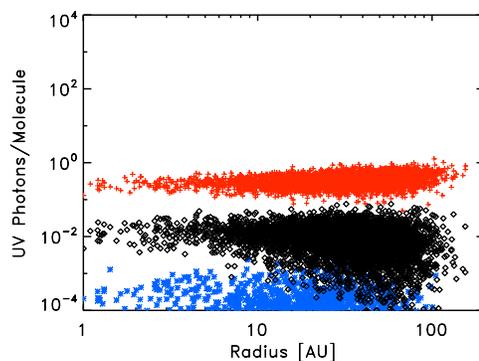
7

Fig. S10. The total UV photons per ice molecule in the surviving 100 μm grains plotted against their final location after 10^6 years of evolution. Colored symbols are as above.
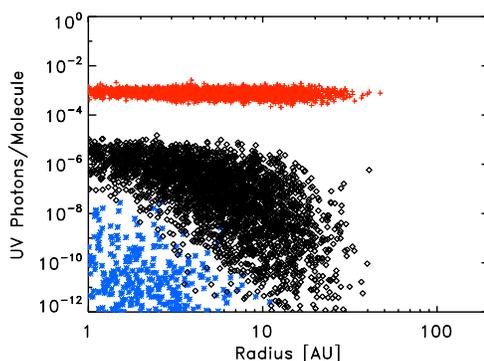

Fig. S11. The total UV photons per ice molecule in the surviving 1 mm grains plotted against their final location after 10^6 years of evolution. Colored symbols are as above.

considered here. Also, note that the average number of total photons seen by a millimeter-sized particle is less than that of the 100 μm particles despite the larger cross-section for intercepting the photons for our nominal and high-opacity cases. This is due to the larger particles having lower vertical diffusivities as given above, and thus not being able to be brought into a region with substantial UV flux.

4. The Production of Organics by Exposure of Mixed Molecular Ices to Radiation

Various aspects of the production of organic compounds during the radiation processing of mixed molecular ices of astrophysical-interest have been under study using laboratory simulations for well over 30 years (*4-10, 37-41*). In general, these laboratory studies attempt to create ices under conditions (temperature, pressure, radiation field, etc.) that are characteristic of specific astrophysical environments like interstellar dense molecular clouds, comets, and planetary and satellite surfaces in the outer Solar System. The ices in these studies have compositions

that vary with the nature of the environment being considered, but generally consist of mixtures of simple molecules like H_2O, CH_3OH, NH_3, HCN, CO, CO_2, and CH. In many astrophysical environments, the most abundant component of the ice is H2O. In some cases, more complex molecule that are known to be present in space, for example polycyclic aromatic hydrocarbons (PAHs) and their variants, are also added to the ices.

Once formed, the ices can be exposed to various kinds of radiation, the two most common being UV photons (e.g. *6*) and energetic protons (e.g., *37*). This ionizing radiation can break bonds between the atoms in the molecules within the ice and results in the production of a variety of reactive ions and radicals. If occupying adjacent sites within the ice, some of these reactive species can interact to form new, more complex molecules even at temperatures as low as 10 K. However, many of these reactive species are trapped within the surrounding ice matrix and cannot react until they are mobilized by phase transitions or ice sublimation when the ice is warmed (e.g. *6*).

In typical experiments, warming of the irradiated ices to room temperature results in the sublimation loss of all the original unaltered ice components, as well as some of the more volatile photoproducts like ethanol (e.g., *6*). However, a significant number of new photoproducts are sufficiently non-volatile to remain behind as an organic residue on the sample substrate. These residues can be removed from the sample substrate and subjected to a variety of chemical analyses including techniques like infrared spectroscopy, High Performance Liquid Chromatography (HPLC), Gas Chromatography with Mass Spectrometry (GCMS), and laser desorption-laser ionization mass spectrometry (L2MS).

This photo-induced chemistry is found to be quite robust in the sense that the production of specific new species is often only weakly dependent on the temperature of the ice during irradiation, the type of radiation used, the rate at which the ice is warmed, or the precise composition of the ice. For example, parallel studies of ices containing H_2O, CH_3OH, NH_3, and CO in concentrations relevant to dense interstellar clouds yielded very similar organic residues independent of whether the ionizing radiation was UV photons or energetic protons (*40*). Similarly, such processing results in the production of amino acids independent of whether the N in the ice is originally in the form of NH_3 or HCN (*41*). This is largely due to the stochastic nature of the process that creates more complex species by reacting a limited suite of simpler ions and radicals. The primary requirements for this type of chemistry are that temperatures be low enough to condense the relevant starting molecules, the radiation be energetic enough to break bonds within the starting molecules in the ice (UV or higher energy photons), and the ice components contain the needed elements (primarily C, N, O, and H). The *relative* production efficiencies of different products is somewhat more dependent on experimental details, but are still rather insensitive to variations in ice temperature, type of radiation, and ice warming rate.

Such studies have demonstrated that radiation processing of ices made up of even simple molecules can result in the production of considerably more complex organic species, many of which are of astrobiological interest. A partial list of examples include:

- *Amino acids* – The amino acids, particularly the simpler ones like glycine and alanine, are produced by the irradiation of virtually any ice that contains a starting mixture of

molecules that, combined, contain C, N, O, and H (*8,9,41,42*).

- *Amphiphiles* – The UV irradiation of dense interstellar cloud ice analogs containing H_2O, CH_3OH, NH_3, and CO produce amphiphilic compounds that are capable, when placed in liquid water, of spontaneously producing membranes and vesicles (*43*). Such materials may have important consequences for the origin of life (*44*).

- *Quinones* – In ices that contain PAHs, irradiation can result in the addition of many kinds of chemical functional groups to the edges of the PAHs (*45,46*). Addition of oxygen atoms results in the production of aromatic alcohols, ethers, and quinones (*7*), molecules of considerable astrobiological interest.

- *Nucleobases* – Just as chemical side groups can be added to PAHs, they can be added to aromatic molecules that contain N within their skeletal rings. For example, recent studies of the irradiation of pyrimidine, a molecule found in meteorites, in ices has demonstrated the production of the nucleobases uracil (*47*).

The efficiency of organic production by the process of ice irradiation is currently not fully constrained. The efficiency of specific molecules has only been determined in a few cases. For example, the work of Bernstein et al. (*8*) showed that the irradiation of ices containing H_2O, CH_3OH, CO, NH_3, and HCN yielded a single amino acid for every $\sim 10^4$ UV photons. However, amino acids represent only a small portion of the organic residues produced and this therefore represents an extreme lower limit to total organic production by this process.

Estimates of total organic production can be made by taking IR spectra of the residues and using band strengths to establish the column densities of various chemical functional groups in the residue. This approach provides a better estimate of the total amount of organics produced and demonstrates that typical experiments designed to match the radiation doses expected in dense interstellar molecular clouds result in conversion of up to 7% of the original ice materials into more complex organics (*6,38*). Comparison of the total number of UV photons hitting the sample with the total number of new functional groups produced indicates quantum efficiencies that range from 0.25% (*6*) up to 1-3% (*38*). We use the more conservative value of 0.25% in the discussion of the main paper.

It should be noted, however, that different elements in the ice are incorporated into the residues with different overall efficiencies. For example, the work of Bernstein et al. (*6*) showed that the uptake of elements from ices containing H_2O, CH_3OH, CO, and NH_3 into the resulting residues varied from as low as 0.5% for oxygen to as high as 45% for N, with the residue accounting for 7% of the C, N, and O atoms in the original ice overall. Thus, it is clear that the production of organics from the irradiation of ices will not increase linearly with radiation dose forever. At some point the production will be limited by the exhaustion of specific starting materials. In addition, at higher doses it is likely that some form of equilibrium will be reached between the production of new organics and the disruption and alteration of previously made organics. Since our model indicates ices in the protosolar disk should receive much higher radiation doses than used in the laboratory simulations of interstellar clouds, and we use the

more conservative quantum efficiency of 0.25%, we expect protosolar processing to produce even more organics than seen in the lab simulations of dense clouds. However, the upperlimit on production is poorly quantified because the much higher doses predicted by the model have yet to be thoroughly examined in the laboratory.

In summary, there is ample evidence that radiation processing of mixed molecular ices of astrophysical relevance results in the production of more complex organic compounds, many of which are of astrobiological interest. This chemistry is robust in the sense that it is expected to occur in a wide variety of astrophysical environments and to be relatively insensitive to environmental conditions like temperature, type of radiation, and exact ice composition. Photolytic processing of ices during the disk evolution described in our model would therefore be expected to result in the production of a wide variety of new organic compounds that would potentially be available for delivery to the surface so of planets where they could play a role in the origin of life.

References

1. E.T. Peltzer *et al. Advances in Space Research* **4**, 69 (1984).

2. J.A. Nuth, N.M. Johnson, S. Manning *Astrophysical Journal* **673**, L225 (2008).

3. S.A. Sandford, M.P. Bernstein, J.P. Dworkin, *Meteoritics and Planetary Science* **36**, 1117 (2001).

4. W. Hagen, L.J. Allamandola, J.M. Greenberg, *Astrophysics and Space Science* **65**, 215 (1979).

5. W.A. Schutte, L.J. Allamandola, S.A. Sandford, *Advances in Space Research* **12**, 47 (1992).

6. M.P. Bernstein *et al. Astrophys. J.* **454**, 327 (1995).

7. M.P. Bernstein *et al. Science* **283**, 1135 (1999).

8. M.P. Bernstein *et al. Nature* **416**, 401 (2002).

9. G.M. Muñoz Caro *et al.*, *Nature* **416**, 403 (2002).

10. M. Nuevo *et al. Advances in Space Research* **48**, 1126 (2011).

11. E.I. Chiang, P. Goldreich, *Astrophys.l J.* **490**, 368 (1997)

12. J.S. Carr, J.R. Najita, *Science* **319**, 1504 (2008).

13. F.J. Ciesla, *Astrophys. J.* **723**, 514 (2010).

14. F.J. Ciesla, *Astrophys. J.* **740**, 9 (2011).

15. S. Charnoz, *et al.*, *Astrophys. J.* **737**, 33 (2011).

16. Materials and Methods are described in the Supporting online Material.

17. F.J. Ciesla, J.N. Cuzzi, *Icarus* **1818**, 178 (2006).

18. T. Sano *et al.*, *Astrophys. J.* **543**, 486 (2000).

19. L. Hartmann, *et al. Astrophys J.* **495**, 385 (1998).

20. S.A. Sandford, *et al. Science* **314**, 720 (2006).

21. K. Nakamura-Messenger *et al. Science* **314**, 1439 (2006).

22. K. Lodders, *Astrophys. J.* **591**, 1220 (2003).

23. K. Willacy, *Astrophys J.* **660**, 441 (2007).

24. Z. Zhu, L. Hartmann, C. Gammie, *Astrophys. J.* **694**, 1045 (2009).

25. H.J. Habing, *Bulletin of the Astronomical Institutes of the Netherlands* **19**, 421 (1968).

26. K. Öberg, *et al.*, *Astrophys. J.* **693**, 1209 (2009).

27. T.J. Bethell, E.A. Bergin, *Astrophys. J.* **739**, 78 (2011).

28. F.C. Adams *et al.*, *Astrophys. J.* **641**, 504 (2006).

29. H.B. Throop, *Icarus* **212**, 885 (2011).

30. S.J. Weidenschilling, *Icarus* **60**, 553 (1984).

31. P. Woitke, I. Kamp, W.-F. Thi, *Astron Astrophys.* **501**, 383 (2009).

32. J.E. Pringle, *Ann. Rev. Astron. Astrophys.* **19**, 137, (1981).

33. S.J. Weidenschilling *Mon. Not. R. Ast. Soc.* **180**, 57, (1977).

34. A.N. Youdin, Y. Lithwick *Icarus* **192**, 588, (2007).

35. A. Johansen, H. Klahr, A.J. Mee, *Mon. Not. R. Ast. Soc.* **370**, 71, (2006).

36. R. Alexander, *New Ast. Rev.* **52**, 60, (2008).

37. M.H. Moore, B. Donn, R. Khanna, M.F. A'Hearn, *Icarus* **54**, 388 (1983).

38. L.J. Allamandola, S.A. Sandford, G. Valero, *Icarus* **76**, 225 (1988).

39. H. Cottin, C. Szopa, M. H. Moore, *Astrophys. J.* **561**, L139 (2001).

40. P.A. Gerakines, M.H. Moore, R.L. Hudson, *J. Geophys. Res.* **106**, 33381 (2001).

41. J.E. Elsila, J.D. Dworkin, M.P. Bernstein, S.A. Sandford, *Astrophys. J.* **660**, 911 (2007).

42. M. Nuevo, G. Auger, D. Blanot, L. d'Hendecourt, *Origins of Life and Evolution of Biospheres* **38**, 37 (2008).

43. J.P. Dworkin, D.W. Deamer, S.A. Sandford, L.J. Allamandola, *Proc. Nat. Acad. Sci. USA* **98**, 815 (2001).

44. D. Deamer, J.P. Dworkin, S.A. Sandford, M.P. Bernstein, L.J. Allamandola, *Astrobiology* **2**, 371 (2002).

45. M.P. Bernstein, J.E. Elsila, J.P. Dworkin, S.A. Sandford, L.J. Allamandola, R.N. Zare, *Astrophys. J.* **576**, 1115 (2002).

46. M.P. Bernstein, M.H. Moore, J.E. Elsila, S.A. Sandford, L.J. Allamandola, R.N. Zare, *Astrophys. J.* **582**, L25 (2003).

47. M. Nuevo, S.N. Milam, S.A. Sandford, J.E. Elsila, J.P. Dworkin, *Astrobiology* **9**, 683 (2009).

References and Notes

1. E. T. Peltzer, J. L. Bada, G. Schlesinger, S. L. Miller, The chemical conditions on the parent body of the Murchison meteorite: Some conclusions based on amino, hydroxy and dicarboxylic acids. *Adv. Space Res.* **4**, 69 (1984). [doi:10.1016/0273-1177(84)90546-5](doi:10.1016/0273-1177(84)90546-5) Medline

2. J. A. Nuth III, N. M. Johnson, S. Manning, A self-perpetuating catalyst for the production of complex organic molecules in protostellar nebulae. *Astrophys. J.* **673**, L225 (2008). [doi:10.1086/528741](doi:10.1086/528741)

3. S. A. Sandford, M. P. Bernstein, J. P. Dworkin, Assessment of the interstellar processes leading to deuterium enrichment in meteoritic organics. *Meteorit. Planet. Sci.* **36**, 1117 (2001). [doi:10.1111/j.1945-5100.2001.tb01948.x](doi:10.1111/j.1945-5100.2001.tb01948.x)

4. W. Hagen, L. J. Allamandola, J. M. Greenberg, Interstellar molecule formation in grain mantles: The laboratory analog experiments, results and implications. *Astrophys. Space Sci.* **65**, 215 (1979). [doi:10.1007/BF00643502](doi:10.1007/BF00643502)

5. W. A. Schutte, L. J. Allamandola, S. A. Sandford, Laboratory simulation of the photoprocessing and warm-up of cometary and pre-cometary ices: Production and analysis of complex organic molecules. *Adv. Space Res.* **12**, 47 (1992). [doi:10.1016/0273-1177(92)90152-N](doi:10.1016/0273-1177(92)90152-N) Medline

6. M. P. Bernstein, S. A. Sandford, L. J. Allamandola, S. Chang, M. A. Scharberg, Organic compounds produced by photolysis of realistic interstellar and cometary ice analogs containing methanol. *Astrophys. J.* **454**, 327 (1995). [doi:10.1086/176485](doi:10.1086/176485)

7. M. P. Bernstein *et al.*, UV irradiation of polycyclic aromatic hydrocarbons in ices: Production of alcohols, quinones, and ethers. *Science* **283**, 1135 (1999). doi:10.1126/science.283.5405.1135 Medline

8. M. P. Bernstein, J. P. Dworkin, S. A. Sandford, G. W. Cooper, L. J. Allamandola, Racemic amino acids from the ultraviolet photolysis of interstellar ice analogues. *Nature* **416**, 401 (2002). [doi:10.1038/416401a](doi:10.1038/416401a) Medline

9. G. M. Muñoz Caro *et al.*, Amino acids from ultraviolet irradiation of interstellar ice analogues. *Nature* **416**, 403 (2002). [doi:10.1038/416403a](doi:10.1038/416403a) Medline

10. M. Nuevo *et al.*, XANES analysis of organic residues produced from the UV irradiation of astrophysical ice analogs. *Adv. Space Res.* **48**, 1126 (2011). [doi:10.1016/j.asr.2011.05.020](doi:10.1016/j.asr.2011.05.020)

11. E. I. Chiang, P. Goldreich, Spectral energy distributions of T Tauri stars with passive circumstellar disks. *Astrophys. J.* **490**, 368 (1997). [doi:10.1086/304869](doi:10.1086/304869)

12. J. S. Carr, J. R. Najita, Organic molecules and water in the planet formation region of young circumstellar disks. *Science* **319**, 1504 (2008). doi:10.1126/science.1153807 Medline

13. F. J. Ciesla, Residence times of particles in diffusive protoplanetary disk environments. I. Vertical motions. *Astrophys. J.* **723**, 514 (2010). [doi:10.1088/0004-637X/723/1/514](doi:10.1088/0004-637X/723/1/514)

14. F. J. Ciesla, Residence times of particles in diffusive protoplanetary disk environments. II. Radial motions and applications to dust annealing. *Astrophys. J.* **740**, 9 (2011). doi:10.1088/0004-637X/740/1/9

15. S. Charnoz, L. Fouchet, J. Aleon, M. Moreira, Three-dimensional lagrangian turbulent diffusion of dust grains in a protoplanetary disk: Method and first applications. *Astrophys. J.* **737**, 33 (2011). doi:10.1088/0004-637X/737/1/33

16. Materials and methods are described in the supplementary materials.

17. F. J. Ciesla, J. N. Cuzzi, The evolution of the water distribution in a viscous protoplanetary disk. *Icarus* **1818**, 178 (2006). doi:10.1016/j.icarus.2005.11.009

18. T. Sano, S. M. Miyama, T. Umebayashi, T. Nakano, Magnetorotational instability in protoplanetary disks. II. Ionization state and unstable regions. *Astrophys. J.* **543**, 486 (2000). doi:10.1086/317075

19. L. Hartmann, N. Calvet, E. Gullbring, P. D'Alessio, Accretion and the evolution of T Tauri disks. *Astrophys. J.* **495**, 385 (1998). doi:10.1086/305277

20. S. A. Sandford *et al.*, Organics captured from comet 81P/Wild 2 by the Stardust spacecraft. *Science* **314**, 1720 (2006). doi:10.1126/science.1135841 Medline

21. K. Nakamura-Messenger, S. Messenger, L. P. Keller, S. J. Clemett, M. E. Zolensky, Organic globules in the Tagish Lake meteorite: Remnants of the protosolar disk. *Science* **314**, 1439 (2006). doi:10.1126/science.1132175 Medline

22. K. Lodders, Solar system abundances and condensation temperatures of the elements. *Astrophys. J.* **591**, 1220 (2003). doi:10.1086/375492

23. K. Willacy, The chemistry of multiply deuterated molecules in protoplanetary disks. I. The outer disk. *Astrophys. J.* **660**, 441 (2007). doi:10.1086/512796

24. Z. Zhu, L. Hartmann, C. Gammie, Nonsteady accretion in protostars. *Astrophys. J.* **694**, 1045 (2009). doi:10.1088/0004-637X/694/2/1045

25. H. J. Habing, *Bull. Astron. Inst. Neth.* **19**, 421 (1968).

26. K. Öberg, H. Linnartz, R. Visser, E. F. van Dishoeck, Photodesorption of ices. II. H_2O and D_2O. *Astrophys. J.* **693**, 1209 (2009).

27. T. J. Bethell, E. A. Bergin, The propagation of Lyα in evolving protoplanetary disks. *Astrophys. J.* **739**, 78 (2011). doi:10.1088/0004-637X/739/2/78

28. F. C. Adams, E. M. Proszkow, M. Fatuzzo, P. C. Myers, Early evolution of stellar groups and clusters: Environmental effects on forming planetary systems. *Astrophys. J.* **641**, 504 (2006). doi:10.1086/500393

29. H. B. Throop, UV photolysis, organic molecules in young disks, and the origin of meteoritic amino acids. *Icarus* **212**, 885 (2011). doi:10.1016/j.icarus.2011.01.002

30. S. J. Weidenschilling, Evolution of grains in a turbulent solar nebula. *Icarus* **60**, 553 (1984). doi:10.1016/0019-1035(84)90164-7

31. P. Woitke, I. Kamp, W.-F. Thi, Radiation thermo-chemical models of protoplanetary disks. *Astron. Astrophys.* **501**, 383 (2009). doi:10.1051/0004-6361/200911821

32. J. E. Pringle, Accretion discs in astrophysics. *Annu. Rev. Astron. Astrophys.* **19**, 137 (1981). doi:10.1146/annurev.aa.19.090181.001033

33. S. J. Weidenschilling, *Mon. Not. R. Ast. Soc.* **180**, 57 (1977).

34. A. N. Youdin, Y. Lithwick, Particle stirring in turbulent gas disks: Including orbital oscillations. *Icarus* **192**, 588 (2007). doi:10.1016/j.icarus.2007.07.012

35. A. Johansen, H. Klahr, A. J. Mee, Turbulent diffusion in protoplanetary discs: The effect of an imposed magnetic field. *Mon. Not. R. Astron. Soc.* **370**, 71 (2006). doi:10.1111/j.1745-3933.2006.00191.x

36. R. Alexander, From discs to planetesimals: Evolution of gas and dust discs. *New Astron. Rev.* **52**, 60 (2008). doi:10.1016/j.newar.2008.04.004

37. M. H. Moore, B. Donn, R. Khanna, M. F. A'Hearn, Studies of proton-irradiated cometary-type ice mixtures. *Icarus* **54**, 388 (1983). doi:10.1016/0019-1035(83)90236-1

38. L. J. Allamandola, S. A. Sandford, G. Valero, Photochemical and thermal evolution of interstellar/precometary ice analogs. *Icarus* **76**, 225 (1988). doi:10.1016/0019-1035(88)90070-X

39. H. Cottin, C. Szopa, M. H. Moore, Production of hexamethylenetetramine in photolyzed and irradiated interstellar cometary ice analogs. *Astrophys. J.* **561**, L139 (2001). doi:10.1086/324575

40. P. A. Gerakines, M. H. Moore, R. L. Hudson, Energetic processing of laboratory ice analogs: UV photolysis versus ion bombardment. *J. Geophys. Res.* **106**, 33381 (2001). doi:10.1029/2000JE001320

41. J. E. Elsila, J. D. Dworkin, M. P. Bernstein, M. P. Martin, S. A. Sandford, Mechanisms of amino acid formation in interstellar ice analogs. *Astrophys. J.* **660**, 911 (2007). doi:10.1086/513141

42. M. Nuevo, G. Auger, D. Blanot, L. d'Hendecourt, A detailed study of the amino acids produced from the vacuum UV irradiation of interstellar ice analogs. *Orig. Life Evol. Biosph.* **38**, 37 (2008). doi:10.1007/s11084-007-9117-y Medline

43. J. P. Dworkin, D. W. Deamer, S. A. Sandford, L. J. Allamandola, Self-assembling amphiphilic molecules: Synthesis in simulated interstellar/precometary ices. *Proc. Natl. Acad. Sci. U.S.A.* **98**, 815 (2001). doi:10.1073/pnas.98.3.815 Medline

44. D. Deamer, J. P. Dworkin, S. A. Sandford, M. P. Bernstein, L. J. Allamandola, The first cell membranes. *Astrobiology* **2**, 371 (2002). doi:10.1089/153110702762470482 Medline

45. M. P. Bernstein *et al.*, Side group addition to the polycyclic aromatic hydrocarbon coronene by ultraviolet photolysis in cosmic ice analogs. *Astrophys. J.* **576**, 1115 (2002). doi:10.1086/341863

46. M. P. Bernstein *et al.*, Side group addition to the polycyclic aromatic hydrocarbon coronene by proton irradiation in cosmic ice analogs. *Astrophys. J.* **582**, L25 (2003). doi:10.1086/345941

47. M. Nuevo, S. N. Milam, S. A. Sandford, J. E. Elsila, J. P. Dworkin, Formation of uracil from the ultraviolet photo-irradiation of pyrimidine in pure H$_2$O ices. *Astrobiology* **9**, 683 (2009). [doi:10.1089/ast.2008.0324](doi:10.1089/ast.2008.0324) Medline